

ActTail: Global Activation Sparsity in Large Language Models

Wenwen Hou^{*1} Xinyuan Song^{*2} Shiwei Liu³

Abstract

Activation sparsity is a promising approach for accelerating large language model (LLM) inference by reducing computation and memory movement. However, existing activation sparsity methods typically apply uniform sparsity across projections, ignoring the heterogeneous statistical properties of Transformer weights and thereby amplifying the performance degradation. In this paper, we propose **ActTail**, a TopK magnitude-based activation sparsity method with global activation sparsity allocation grounded in Heavy-Tailed Self-Regularization (HT-SR) theory. Specifically, we capture this heterogeneity via the heavy-tail exponent α computed from each projection’s empirical spectral density (ESD), which is used as a quantitative indicator to assign projection-specific sparsity budgets. Importantly, we provide a theoretical analysis that establishes an explicit relationship between the activation sparsity ratio and the heavy-tail exponent α under the HT-SR regime, offering principled guidance for sparsity allocation beyond heuristic design. Experiments on LLaMA and Mistral models show that our method improves both perplexity and downstream task performance at high sparsity compared to uniform allocation. At 80% sparsity, perplexity is reduced by 21.8% on LLaMA-2-7B, 40.1% on LLaMA-2-13B, and 9.4% on Mistral-7B.

1. Introduction

Modern large language models have grown to tens or even hundreds of billions of parameters, leading to substantial memory and computational overhead during inference and posing challenges for deployment in settings with limited resources (Kaplan et al., 2020; Hoffmann et al., 2022; Touvron et al., 2023a; Yang et al., 2025). To address these challenges,

¹The Hong Kong University of Science and Technology (Guangzhou) ²Emory University ³ELLIS Institute Tübingen & Max Planck Institute for Intelligent Systems. Correspondence to: Shiwei Liu <sliu@tue.ellis.eu>.

Preprint. March 16, 2026.

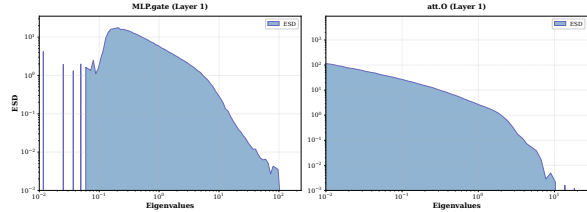


Figure 1. Eigenvalue spectral density (ESD) for MLP gate projection and attention output projection in Layer 1 of Llama2-13B model.

a broad class of efficiency techniques including weight pruning (Frantar & Alistarh, 2023; An et al., 2024; Ashkboos et al., 2024; Ling et al., 2024; Sun et al., 2024; Shen et al., 2025), and low rank decomposition (Wang et al., 2025; Huang et al., 2025) has been proposed to reduce model size and computational cost. Weight pruning typically eliminates parameters or units (e.g., neurons or channels) deemed unimportant according to predefined importance metrics, resulting in sparse weight matrices. Low-rank decomposition, on the other hand, reduces model complexity by factorizing weight matrices into low-rank components. Once applied, these methods induce a static model structure, whereby all input instances are processed using the same sparsity pattern or low-rank factorization. Therefore, these methods often suffer from accuracy loss and reduced robustness at high compression rates, which limits their effectiveness in practice. Recently, a complementary line of work on contextual activation sparsity has emerged (Liu et al., 2023; Lee et al., 2024; Zhang et al., 2025; Liu et al., 2025b;a) inspired by lazy neuron phenomenon, which exploits input-dependent sparsity in hidden states. Because channels associated with zero valued activations do not participate in computation, both arithmetic operations and memory movement can be reduced by skipping the corresponding weight channels during memory access, enabling efficient inference under channel wise sparsity.

Despite their success, most activation sparsity methods (Liu et al., 2025a;b) rely on either uniform rules or greedy search to determine sparsity rates across layers and projections. Uniform sparsity ignores the heterogeneous importance of different components and often leads to unnecessary accuracy loss at high sparsity levels, while greedy procedures lack theoretical guidance and incur substantial computa-

tional overhead. To derive more effective and theoretically guided sparsity allocation, we leverage insights from Heavy Tailed Self Regularization theory (Martin & Mahoney, 2017; 2021b; 2019; 2020; He et al., 2025). HT-SR theory studies trained weight matrices through empirical spectral densities (ESDs) of the corresponding correlation matrices (See Figure 1), connecting spectral structure to matrix-level training quality. Building on this property, we developed an HT-SR theory guided activation sparsity scheme.

This work focuses on input activation sparsity in Transformer projections, including the linear projections in self-attention and the feed-forward network (FFN). Input sparsity is induced using topK selection on the layer input hidden state, which keeps only the K largest entries and sets the rest to zero. Hence, the corresponding weight channels are unused and can be skipped. The heavy tail exponent α from Heavy Tailed Self Regularization theory is used to guide sparsity at the projection level. Specifically, each projection’s α is mapped to a projection specific sparsity ratio, which determines its topK retention rate during inference. In summary, the contributions are as follows:

- A data-independent activation sparsity method based on topK sparsification is introduced, which induces input activation sparsity without relying on calibration data.
- We establish a theoretical connection between Heavy Tailed Self Regularization and activation sparsity, showing how heavy tailed spectral statistics predict the sparsifiability of different projections and support projection level sparsity allocation.
- Extensive experiments on the LLaMA2 family, Mistral 7B, and Qwen1.5 7B demonstrate that ActTail consistently outperforms uniform allocation, improving both perplexity and downstream task performance at high sparsity.

Overall, ActTail offers a principled and practical framework for activation sparsity in large language models, combining theoretical insights from heavy-tailed self-regularization with efficient topK inference-time sparsification. By adapting sparsity to the intrinsic statistical properties of individual projections, ActTail achieves substantial efficiency gains while maintaining strong performance across perplexity and downstream benchmarks.

2. Related Work

Activation Sparsity in LLMs. Activation sparsity arises when a substantial fraction of a model’s hidden-state entries are zero, and can be viewed as a form of conditional computation that selectively activates parts of the network (Bengio et al., 2016). Such sparsity naturally emerges in the intermediate representations of ReLU-based MLP blocks (Li et al.,

2023). Prior work has demonstrated that activation sparsity can be exploited to accelerate LLM inference by avoiding unnecessary computation and memory transfer. Liu et al. (2023) leverages zero-valued activations to skip transferring corresponding weight channels to GPU registers during decoding, while Song et al. (2024) and Alizadeh et al. (2024) extend this idea to CPU offloading, significantly reducing data movement between CPU and GPU memory. However, modern leading LLMs increasingly adopt non-ReLU activation functions, such as SwiGLU (So et al., 2021), which do not inherently produce sparse activations (Touvron et al., 2023b; Qwen Team, 2024).

Recent work focuses on inducing activation sparsity in modern LLM architectures that no longer rely on ReLU-based MLPs. Mirzadeh et al. (2023) reintroduce sparsity by replacing SiLU or GeLU with ReLU followed by continued large-scale pretraining, while Zhang et al. (2024) systematically study alternative activations and identify Squared ReLU as an effective replacement. In the training-free setting, Lee et al. (2024) induce activation sparsity in SwiGLU-based LLMs by applying magnitude-based thresholding to the gating output. Liu et al. (2025a) extends magnitude-based activation sparsity to the input activations of both self-attention and MLP blocks. More recently, Liu et al. (2025b) introduce layerwise orthogonal rotations to transform input activations into a space that is more amenable to sparsification, enabling consistent model-level sparsity and reliable wall-clock acceleration without additional training. Shrestha et al. (2025) propose Polar Sparsity, which reveals a shift in sparsity efficiency from MLP layers to attention layers as batch size and sequence length increase.

Heavy-Tailed Self-Regularization Theory. Heavy-Tailed Self-Regularization (HT-SR) theory studies the empirical spectral density (ESD) of trained neural network weight matrices and relates their spectral structure to training quality, drawing on insights from statistical physics and random matrix theory (Martin & Mahoney, 2021b; Couillet & Liao, 2022). Under HT-SR theory, heavier-tailed ESDs of weight matrices indicate stronger optimization-induced correlations and higher layer training quality (Martin & Mahoney, 2019). Recently, HT-SR has been successfully applied across a range of model analysis and optimization tasks (Lu et al., 2024; He et al., 2025). In model selection, HT-SR metrics have been shown to reliably rank pretrained networks and checkpoints by quality without access to training data (Martin et al., 2021; Yang et al., 2023). In module-wise adaptive training, heavy-tailed spectral statistics have been used to diagnose layer-wise training imbalance and to guide adaptive optimization strategies (Zhou et al., 2023).

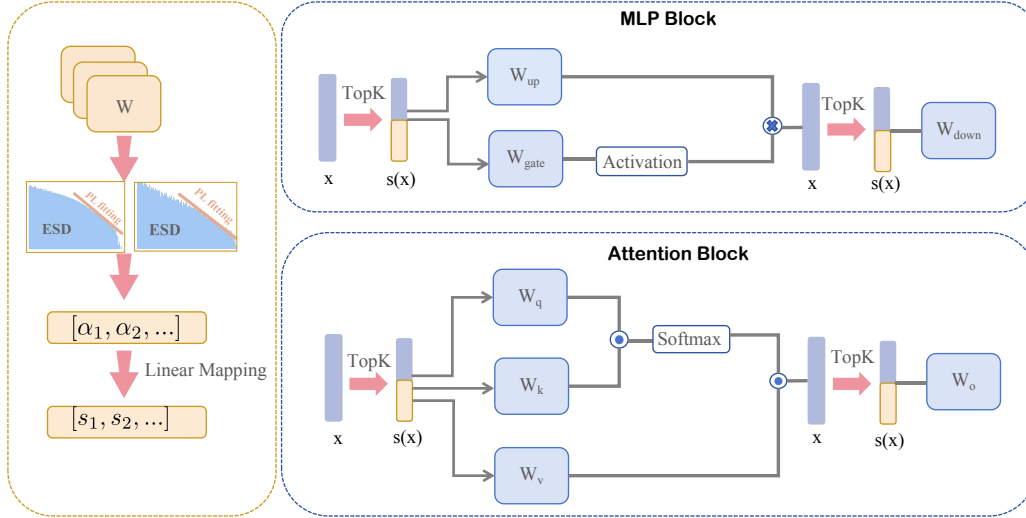


Figure 2. Overview of the ActTail workflow. ActTail first estimates heavy-tailed exponents from the empirical spectral density (ESD) of each projection, maps them to projection-level sparsity ratios via a linear rule, and applies TopK activation sparsity during inference.

3. Methodology

3.1. Notation

We consider a Transformer with L layers and focus on inference-time acceleration at the decoding stage. At each decoding step, for each linear projection p in layer ℓ , the projection receives an input activation $\mathbf{h}^{(\ell,p)} \in \mathbb{R}^{d_{\text{in}}^{(p)}}$. The set of projections is indexed by $p \in \mathcal{P} = \{\text{q, k, v, o, gate, up, down}\}$.

Each projection is parameterized by a weight matrix $\mathbf{W}^{(\ell,p)} \in \mathbb{R}^{d_{\text{out}}^{(p)} \times d_{\text{in}}^{(p)}}$. Input activation sparsity is applied during decoding via a binary mask $\mathbf{m}^{(\ell,p)} \in \{0, 1\}^{d_{\text{in}}^{(p)}}$, producing a sparsified projection input $\tilde{\mathbf{h}}^{(\ell,p)} = \mathbf{m}^{(\ell,p)} \odot \mathbf{h}^{(\ell,p)}$ and the corresponding projection output $\mathbf{a}^{(\ell,p)} = \mathbf{W}^{(\ell,p)} \tilde{\mathbf{h}}^{(\ell,p)}$. The sparsity ratio $s^{(\ell,p)} \in [0, 1]$ is defined as the fraction of zero entries in $\mathbf{m}^{(\ell,p)}$.

For each projection p in layer ℓ , the correlation matrix is $\mathbf{X}^{(\ell,p)} = \mathbf{W}^{(\ell,p)\top} \mathbf{W}^{(\ell,p)}$. Let $\{\lambda_j\}_{j=1}^n$ be the eigenvalues of $\mathbf{X}^{(\ell,p)}$ and the empirical spectral density (ESD) is formulated as $\mu_{\mathbf{X}^{(\ell,p)}} := \frac{1}{n} \sum_{j=1}^n \delta_{\lambda_j}$.

For the ESD $\mu_{\mathbf{X}^{(\ell,p)}}$,

$$p(\lambda) \propto \lambda^{-\alpha^{(\ell,p)}}, \quad \lambda_{\min}^{(\ell,p)} < \lambda < \lambda_{\max}^{(\ell,p)}, \quad (1)$$

is the fitted power-law density function.

3.2. TopK Input Activation Sparsity during Inference

In this work, we focus on input activation sparsity for the decoding stage, targeting the linear projections in each Transformer layer. For projection p in layer ℓ , a binary mask $\mathbf{m}^{(\ell,p)}$ is applied to the hidden state $\mathbf{h}^{(\ell)}$ before the pro-

jection. If an entry of $\mathbf{h}^{(\ell)}$ is zero, then the corresponding column of $\mathbf{W}^{(\ell,p)}$ is unused and can be skipped, reducing both computation and weight memory access. Formally,

$$\mathbf{a}^{(\ell,p)} = \mathbf{W}^{(\ell,p)} (\mathbf{m}^{(\ell,p)} \odot \mathbf{h}^{(\ell)}) = \mathbf{W}^{(\ell,p)} \tilde{\mathbf{h}}^{(\ell,p)}, \quad (2)$$

where the sparsity ratio $s^{(\ell,p)}$ is the fraction of zeros in $\mathbf{m}^{(\ell,p)}$.

The mask $\mathbf{m}^{(\ell,p)}$ is constructed in a magnitude based way. Prior work such as (Liu et al., 2025a) uses thresholding, which zeros out entries whose magnitudes fall below a learned threshold. However, it depends on calibration data and does not guarantee an exact sparsity ratio. Instead, we propose a TopK rule to build $\mathbf{m}^{(\ell,p)}$ by keeping the $K^{(\ell,p)}$ largest-magnitude entries of $\mathbf{h}^{(\ell)}$ and masking out the rest. Unlike thresholding, TopK fixes the number of active dimensions, so the sparsity ratio is explicitly controlled as

$$s^{(\ell,p)} = 1 - \frac{K^{(\ell,p)}}{d_{\text{in}}^{(p)}}. \quad (3)$$

This provides stable, data-independent sparsity control during inference.

3.3. Heavy-Tailed Self-Regularization Theory (HT-SR)

Motivation: from HT-SR theory to activation sparsity. Given a projection weight matrix $\mathbf{W}^{(\ell,p)}$, HT-SR studies the empirical spectral density (ESD) of its correlation matrix $\Sigma^{(\ell,p)} = \mathbf{W}^{(\ell,p)\top} \mathbf{W}^{(\ell,p)}$. HT-SR theory links the spectral structure of trained weight matrices to the quality of learned representations (Martin & Mahoney, 2021a; 2020; Martin et al., 2021; He et al., 2025). This connection arises because the ESD reflects the correlation structure encoded in $\mathbf{W}^{(\ell,p)}$.

Method	LLaMA2 7B	LLaMA2 13B	Mistral 7B	Qwen1.5 7B
Dense (0%)	5.11	4.57	4.91	7.36
TEAL _{Top-K} (60%)	5.94	5.15	5.57	8.47
ActTail (60%)	5.86	5.14	5.57	8.42
TEAL _{Top-K} (70%)	9.35	6.88	7.84	12.28
ActTail (70%)	8.09	6.25	7.70	11.40
TEAL _{Top-K} (80%)	36.37	29.66	23.87	57.24
ActTail (80%)	28.43	17.76	21.63	56.21

Table 1. Perplexity on WikiText2 under different activation sparsity levels. Lower is better.

Effective training induces stronger correlations, which manifest as heavy-tailed spectral behavior and indicate higher matrix training quality.

This perspective provides a natural motivation for input activation sparsity. Input sparsification removes a subset of hidden-state dimensions before multiplying by $\mathbf{W}^{(\ell,p)}$, which is equivalent to skipping the corresponding columns of $\mathbf{W}^{(\ell,p)}$ during decoding. According to HT-SR theory, projections with more heavy-tailed ESDs tend to encode stronger learned structure, so they should be sparsified more conservatively. Conversely, projections with lighter-tailed spectra can tolerate higher input sparsity. Therefore, HT-SR theory offers a principled signal for allocating activation sparsity across projections, replacing uniform rules or costly search with a theory-guided allocation strategy.

Heavy-tailed Metric. To quantify the heavy-tailedness of ESDs, HT-SR adopts a *shape metric* based on a power-law fit. Given the ESD of the correlation matrix $\mathbf{X}^{(\ell,p)}$, we fit a power-law (PL) on the interval $(\lambda_{\min}^{(\ell,p)}, \lambda_{\max}^{(\ell,p)})$, taking the form

$$p(\lambda) \propto \lambda^{-\alpha^{(\ell,p)}}, \quad \lambda_{\min}^{(\ell,p)} < \lambda < \lambda_{\max}^{(\ell,p)}. \quad (4)$$

Here, $p(\lambda)$ denotes the density of eigenvalues λ within the specified interval. The exponent $\alpha^{(\ell,p)}$ provides a quantitative measure of the ESD’s tail heaviness. In practice, we compute $\alpha^{(\ell,p)}$ for each layer ℓ and module p (e.g., attention/MLP projections).

For estimating α , we apply the Hill estimator (Hill, 1975; Xiao et al., 2023; Zhou et al., 2023), denoted as PL_Alpha_Hill,

$$\text{PL_Alpha_Hill} = 1 + \frac{k}{\sum_{i=1}^k \ln \left(\frac{\lambda_{n-i+1}}{\lambda_{n-k}} \right)}, \quad (5)$$

where $\{\lambda_i\}_{i=1}^n$ are the eigenvalues in ascending order and k controls the lower cutoff used for tail fitting. As shown in Figure 3, the estimated α values vary across both depth

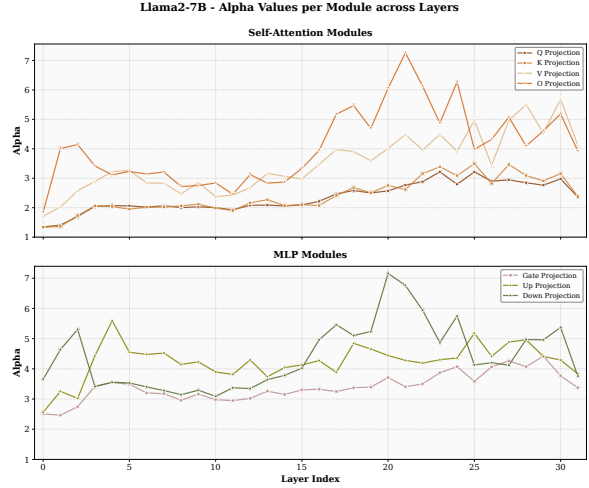


Figure 3. Power-law exponents α (Hill estimator) of the ESDs for different modules across layers in LLaMA2-7B. Smaller α indicates heavier tails.

and projection types, indicating heterogeneous heavy-tailed behavior in different components of the Transformer.

3.4. ActTail: Global Activation Sparsity Allocation

Motivated by the observed spectral diversity across projections, ActTail therefore uses each projection’s heavy-tailed exponent $\alpha^{(\ell,p)}$ to set its TopK input sparsity ratio $s^{(\ell,p)}$. ActTail computes $\alpha^{(\ell,p)}$ from the ESD of the correlation matrix $\mathbf{X}^{(\ell,p)} = \mathbf{W}^{(\ell,p)\top} \mathbf{W}^{(\ell,p)}$ for each projection weight matrix $\mathbf{W}^{(\ell,p)}$. Then, we map the heavy-tailed exponents $\alpha^{(\ell,p)}$ of all projections to projection-level sparsity ratios through a monotone affine function. Figure 2 provides an overview of the ActTail workflow, from estimating heavy-tailed exponents to allocating projection-level sparsity and applying TopK gating during inference.

$$s^{(\ell,p)} = \eta \left[\frac{\alpha^{(\ell,p)} - \alpha_{\min}}{\alpha_{\max} - \alpha_{\min}} (s_2 - s_1) + s_1 \right], \quad (6)$$

where α_{\min} and α_{\max} are the minimum and maximum values of $\alpha^{(\ell,p)}$ across all projections, and (s_1, s_2) controls the degree of non-uniformity. The normalization factor η rescales all projection sparsities to satisfy a target global sparsity level S , i.e., $\sum_{(\ell,p)} s^{(\ell,p)} d^{(\ell,p)} = S \sum_{(\ell,p)} d^{(\ell,p)}$, where $d^{(\ell,p)}$ denotes the parameter count of $\mathbf{W}^{(\ell,p)}$.

4. Theoretical Analysis

Section 3 motivates ActTail from the perspective of Heavy-Tailed Self-Regularization (HT-SR) theory and introduces a linear mapping from projection-level heavy-tail exponents to sparsity ratios. However, it lacks a theoretical explanation why projections with more heavy-tailed spectra should

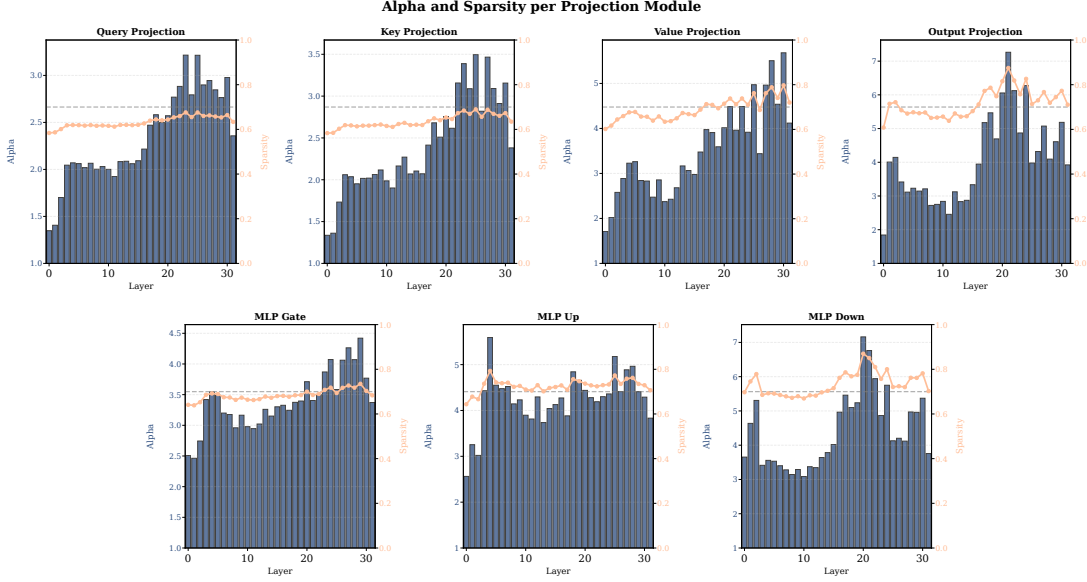


Figure 4. Alpha and sparsity per projection module across layers.

admit more aggressive TopK activation sparsification. In this section, we provide a rigorous theoretical analysis establishing a formal link between heavy-tailed spectral behavior and activation sparsity under TopK sparsity.

To prove that heavy-tailed spectra lead to activation sparsity, we first establish a generic TopK approximation guarantee. Lemma 4.1 provides an ℓ_2 best K -term (TopK) approximation bound in terms of the weak- ℓ_p (Lorentz) quasi-norm, and will serve as the first step of our proof chain.

Lemma 4.1 (ℓ_2 Best K -term approximation). *Let $d \geq 1$ and $p \in (2, \infty)$. For $y \in \mathbb{R}^d$, let $|y|_{(1)} \geq \dots \geq |y|_{(d)}$ denote the decreasing rearrangement of $\{|y_1|, \dots, |y_d|\}$. Let $T_K(y)$ be the TopK truncation that keeps the K largest-magnitude coordinates of y and sets the rest to zero. Then for any $K \in \{1, \dots, d\}$,*

$$\|y - T_K(y)\|_2 \leq C_p \|y\|_{p, \infty} K^{\frac{1}{2} - \frac{1}{p}}, \quad (7)$$

where $C_p > 0$. $\|\cdot\|_{p, \infty}$ is the weak- ℓ_p (Lorentz) quasi-norm $\|y\|_{p, \infty} := \sup_{1 \leq j \leq d} j^{1/p} |y|_{(j)}$.

Proof. By Stechkin inequality (Jahn & Ullrich, 2021) or optimal K -term approximation bound for Lorentz spaces (Devore, 1998), we rearrange the bound

$$|y|_{(j)} \leq \|y\|_{p, \infty} j^{-1/p} \quad (8)$$

then computes

$$\begin{aligned} \|y - T_K(y)\|_2^2 &= \sum_{j>K} |y|_{(j)}^2 \leq \|y\|_{p, \infty}^2 \sum_{j>K} j^{-2/p} \\ &\leq \|y\|_{p, \infty}^2 \int_K^\infty t^{-2/p} dt \\ &= \frac{p}{2-p} \|y\|_{p, \infty}^2 K^{1-2/p}. \end{aligned} \quad (9)$$

Taking square roots yields (7) with $C_p = \sqrt{\frac{p}{2-p}}$. \square

Lemma 4.1 quantifies how well a vector y can be approximated in ℓ_2 by its TopK truncation $T_K(y)$, with the approximation quality controlled by the weak- ℓ_p quasi-norm $\|y\|_{p, \infty}$. The theorem upper-bounds the ℓ_2 error of TopK truncation by $\|y - T_K(y)\|_2 \leq C_p \|y\|_{p, \infty} K^{\frac{1}{2} - \frac{1}{p}}$. In particular, if $y \in \ell_{p, \infty}$ (i.e., $\|y\|_{p, \infty} < \infty$), then the TopK error in ℓ_2 decays as $K^{1/2-1/p}$.

To apply Lemma 4.1, we next relate the weak- ℓ_p behavior of $y = Wx$ to the heavy-tail ESD exponent α of $X = W^\top W$ via spectral energy concentration. Lemma 4.2 connects the fitted heavy-tail exponent α of the ESD to a concrete energy-capture law for the spectrum. It shows how the fraction of spectral energy contained in the top- qn eigenvalues scales with q .

Lemma 4.2 (power-law tail integral). *Let $X \in \mathbb{R}^{n \times n}$ be positive semi-definite matrix (PSD) with eigenvalues $\lambda_1 \geq \dots \geq \lambda_n \geq 0$. Assume the ESD of X follows a power-law tail with exponent $\alpha > 2$, there exist constants $c_0, c_1 > 0$ and a smooth function $L(\cdot)$ such that for large t ,*

$$\mathbb{P}(\Lambda \geq t) = c_0 t^{1-\alpha} L(t) \quad (\Lambda \sim \text{ESD of } X), \quad (10)$$

Moreover, Define the top- q spectral energy capture ratio for $q \in (0, 1)$:

$$R(q) := \frac{\sum_{j \leq qn} \lambda_j}{\sum_{j=1}^n \lambda_j}. \quad (11)$$

Then, for q in the regime where the power-law fit holds, one has the scaling law

$$R(q) \asymp q^{\frac{\alpha-2}{\alpha-1}}, \quad (12)$$

Proof. Let $\bar{F}(t) := \mathbb{P}(\Lambda \geq t)$. We have:

$$\bar{F}(t) = c_0 t^{1-\alpha} L(t). \quad (13)$$

It means \bar{F} is power law distribution of index $(1 - \alpha)$. Let τ_q be the upper-tail quantile defined by $\bar{F}(\tau_q) = q$. We now justify the scaling $\tau_q \asymp q^{-1/(\alpha-1)}$ under the regularly varying tail assumption.

$$q = c_0 \tau_q^{1-\alpha} L(\tau_q). \quad (14)$$

Rearranging (14) gives

$$\tau_q^{\alpha-1} = \frac{c_0 L(\tau_q)}{q}. \quad (15)$$

Since $L(\cdot)$ is smooth, the factor $L(\tau_q)$ changes only sub-polynomially with τ_q . In particular, there exists another smooth function $\tilde{L}(\cdot)$ (i.e. the de Bruijn conjugate (Bingham et al., 1987) of L) such that the asymptotic inverse of $t \mapsto t^{1-\alpha} L(t)$ satisfies

$$\tau_q = \left(\frac{c_0}{q}\right)^{\frac{1}{\alpha-1}} \tilde{L}\left(\frac{1}{q}\right), \quad q \downarrow 0, \quad (16)$$

and therefore

$$\tau_q \asymp q^{-\frac{1}{\alpha-1}} \quad \text{as } q \downarrow 0, \quad (17)$$

where the \asymp relation hides only multiplicative constants and the factor $\tilde{L}(1/q)$.

Now consider the upper-tail first moment

$$M_1(t) := \mathbb{E}[\Lambda \mathbf{1}\{\Lambda \geq t\}]. \quad (18)$$

By Karamata's theorem (Resnick, 1987) for power law tails, since $\alpha > 2$,

$$M_1(t) \asymp t^{2-\alpha} L(t), \quad (19)$$

again up to multiplicative constants. Therefore,

$$\frac{\mathbb{E}[\Lambda \mathbf{1}\{\Lambda \geq \tau_q\}]}{\mathbb{E}[\Lambda]} \asymp \tau_q^{2-\alpha} \asymp \left(q^{-1/(\alpha-1)}\right)^{2-\alpha} = q^{\frac{\alpha-2}{\alpha-1}}. \quad (20)$$

Finally, the Riemann-sum/quantile approximation hypothesis (van der Vaart, 1998) transfers this distributional energy-capture ratio to the discrete ratio $R(q)$, yielding (12). \square

Lemma 4.2 states that under a power-law ESD tail with exponent $\alpha > 2$, the top- q spectral energy capture ratio obeys $R(q) \asymp q^{\frac{\alpha-2}{\alpha-1}}$ in the regime where the fit holds, so α directly controls how quickly spectral energy concentrates into the leading eigenvalues.

Building on this α -dependent spectral concentration, we next show how it transfers to the coordinate magnitudes of $y = Wx$, yielding an explicit α -indexed activation sparsity rule. We now connect the heavy-tailed ESD exponent α to projection-level activation sparsity. Under Assumption 4.3, the key step is to show that the activation $y = Wx$ is weak- $\ell_{p(\alpha)}$ with $p(\alpha) = 2(\alpha - 1)$, which, together with Lemma 4.1, yields an explicit choice of K and hence an explicit sparsity ratio $s(\alpha, \varepsilon)$.

Assumption 4.3. Fix (ℓ, p) and let $W := W^{(\ell, p)} \in \mathbb{R}^{d_{\text{out}} \times d_{\text{in}}}$ and $X := W^\top W$. Let $x \in \mathbb{R}^{d_{\text{in}}}$ be mean-zero, isotropic, and sub-Gaussian with parameter κ , and set $y := Wx$. Assume the ESD of X satisfies the condition in Lemma 4.2 with exponent $\alpha^{(\ell, p)} = \alpha > 2$. Let $V := WW^\top$ and define $v_i := V_{ii} = \text{Var}(y_i)$. There exists a constant $\gamma \geq 1$ such that the decreasing rearrangements satisfy

$$v_{(j)} \leq \gamma \sigma_j^2, \quad \forall j \in \{1, \dots, d_{\text{out}}\}, \quad (21)$$

where $\sigma_1^2 \geq \sigma_2^2 \geq \dots$ are the eigenvalues of V .

Theorem 4.4 (Spectral energy concentration). *Under Assumption 4.3, for any $\delta \in (0, 1)$, with probability at least $1 - \delta$, the activation vector y belongs to a weak- $\ell_{p(\alpha)}$ ball with $p(\alpha) = 2(\alpha - 1)$, in the sense that*

$$|y|_{(j)} \leq C(\kappa, \gamma) \sqrt{\log\left(\frac{d_{\text{out}}}{\delta}\right)} j^{-1/p(\alpha)}, \quad (22)$$

for $\forall j \in \{1, \dots, d_{\text{out}}\}$. Consequently, by Lemma 4.1, for any target tolerance $\varepsilon > 0$, choosing

$$K(\alpha, \varepsilon) \geq \left(\frac{\sqrt{\log(d_{\text{out}}/\delta)}}{\varepsilon}\right)^{\frac{2(\alpha-1)}{\alpha-2}} \quad (23)$$

ensures $\|y - T_{K(\alpha, \varepsilon)}(y)\|_2 \leq \varepsilon$, and the corresponding activation sparsity ratio is $s(\alpha, \varepsilon) = 1 - \frac{K(\alpha, \varepsilon)}{d_{\text{out}}}$.

Proof. For each coordinate i , $y_i = w_i^\top x$, where w_i^\top is the i -th row of W . Since x is sub-Gaussian and isotropic, y_i is sub-Gaussian with variance proxy $\|w_i\|_2^2 = v_i$. By Hanson-Wright inequality (Vershynin, 2018), the rank-one quadratic form $(w_i^\top x)^2 = x^\top (w_i w_i^\top) x$ becomes:

$$\begin{aligned} \mathbb{P}\left(|y_i| \geq t\right) &\leq 2 \exp\left(-c \min\left(\frac{t^2}{\kappa^2 v_i}, \frac{t}{\kappa \sqrt{v_i}}\right)\right) \\ &\leq 2 \exp\left(-c \frac{t^2}{\kappa^2 v_i}\right) \end{aligned} \quad (24)$$

Table 2. Downstream performance under different sparsity levels. Best results at each sparsity level are in **bold**.

Model	Sparsity	Method	Avg.	MMLU	ARC-c	HellaSwag	BOOLQ	PIQA	WinoGrande
LLaMA2-7B	0%	Dense	62.72	45.84	43.43	57.13	77.74	78.07	74.11
	70%	TEAL _{Top-K}	56.02	26.53	28.50	41.84	65.66	70.67	50.36
	70%	ActTail	58.06	27.35	30.97	44.07	66.97	72.25	56.12
	80%	TEAL _{Top-K}	47.87	23.58	19.62	28.97	44.62	60.50	48.78
	80%	ActTail	49.27	25.32	21.08	30.09	56.94	61.92	51.22
LLaMA2-13B	0%	Dense	65.93	55.13	48.46	60.06	80.61	79.05	72.22
	70%	TEAL _{Top-K}	58.06	30.63	33.96	46.51	68.23	72.80	61.40
	70%	ActTail	62.18	36.88	40.27	49.55	72.51	74.10	63.77
	80%	TEAL _{Top-K}	48.73	24.95	20.22	30.62	51.47	63.38	51.78
	80%	ActTail	52.61	26.61	25.51	36.23	64.16	63.22	52.93
Mistral-7B	0%	Dense	69.72	62.65	50.34	61.24	83.64	80.58	73.80
	70%	TEAL _{Top-K}	59.17	30.37	34.30	47.17	67.80	73.23	62.67
	70%	ActTail	59.42	33.20	34.39	46.78	67.49	73.23	64.25
	80%	TEAL _{Top-K}	48.12	24.37	18.77	31.64	44.46	63.60	51.46
	80%	ActTail	49.15	24.70	21.16	32.10	51.72	63.87	50.91
Qwen1.5-7B	0%	Dense	65.78	60.53	40.61	57.80	82.51	78.40	74.90
	70%	TEAL _{Top-K}	54.48	31.99	31.23	43.24	67.06	71.11	53.04
	70%	ActTail	55.85	36.50	32.00	44.66	69.69	70.78	58.25
	80%	TEAL _{Top-K}	53.32	25.84	19.62	30.72	60.73	64.15	50.99
	80%	ActTail	52.47	25.32	21.76	30.77	60.40	61.37	50.91

for all $t > 0$ in the sub-Gaussian range, where $c > 0$ is a constant.

Set

$$t_i := \kappa \sqrt{\frac{v_i}{c} \log\left(\frac{2d_{\text{out}}}{\delta}\right)}. \quad (25)$$

Plugging $t = t_i$ into (24) gives

$$\begin{aligned} \mathbb{P}(|y_i| \geq t_i) &\leq 2 \exp\left(-c \frac{t_i^2}{\kappa^2 v_i}\right) \\ &= 2 \exp\left(-\log\left(\frac{2d_{\text{out}}}{\delta}\right)\right) = \frac{\delta}{d_{\text{out}}}. \end{aligned} \quad (26)$$

Therefore, we have:

$$\mathbb{P}(\exists i \in [d_{\text{out}}] : |y_i| \geq t_i) \leq \sum_{i=1}^{d_{\text{out}}} \mathbb{P}(|y_i| \geq t_i) \leq \delta. \quad (27)$$

With probability at least $1 - \delta$, we have $|y_i| \leq t_i$ for all i simultaneously. Thus we have:

$$|y_i| \leq C_0 \kappa \sqrt{v_i \log\left(\frac{d_{\text{out}}}{\delta}\right)} \quad \forall i. \quad (28)$$

By Lemma 4.2, the eigenvalues of $V = WW^\top$ obeying the same tail exponent α under Assumption 4.3 have a power-law order-statistics behavior on the fitted range, namely

$$\sigma_j^2 \asymp j^{-1/(\alpha-1)} \quad (29)$$

Again by Assumption 4.3 implies

$$v_{(j)} \leq \gamma \sigma_j^2 \leq j^{-1/(\alpha-1)}. \quad (30)$$

Sort the coordinates by magnitude and combine (28) with the bound on $v_{(j)}$:

$$\begin{aligned} |y|_{(j)} &\leq C_0 \kappa \sqrt{v_{(j)} \log\left(\frac{d_{\text{out}}}{\delta}\right)} \\ &\leq \sqrt{\log\left(\frac{d_{\text{out}}}{\delta}\right)} j^{-1/(2(\alpha-1))}. \end{aligned} \quad (31)$$

This is exactly the weak- $\ell_{p(\alpha)}$ condition with $p(\alpha) = 2(\alpha - 1)$. Apply Lemma 4.1 with $p = p(\alpha)$ and $\|y\|_{p,\infty} \leq 1\sqrt{\log(d_{\text{out}}/\delta)}$ to obtain

$$\begin{aligned} \|y - T_K(y)\|_2 &\leq \sqrt{\log\left(\frac{d_{\text{out}}}{\delta}\right)} K^{\frac{1}{2} - \frac{1}{2(\alpha-1)}} \\ &= \sqrt{\log\left(\frac{d_{\text{out}}}{\delta}\right)} K^{\frac{\alpha-2}{2(\alpha-1)}}. \end{aligned} \quad (32)$$

Solving for K to make $\|y - T_K(y)\|_2 \leq \varepsilon$ gives (23):

$$K(\alpha, \varepsilon) \geq \left(\frac{\sqrt{\log(d_{\text{out}}/\delta)}}{\varepsilon}\right)^{\frac{2(\alpha-1)}{\alpha-2}} \quad (33)$$

□

Theorem 4.4 shows that the heavy-tailed spectral exponent α directly determines how aggressively a projection can be sparsified under a fixed error tolerance: via $p(\alpha) = 2(\alpha - 1)$ it controls the decay of activation magnitudes and yields an explicit sparsity ratio $s(\alpha, \varepsilon)$. Therefore, more heavy-tailed spectra (smaller α) permit more aggressive activation sparsity than lighter one (larger α), yielding an α -guided principle for projection-level sparsity allocation. In the following section, we substantiate this insight through comprehensive experimental evaluations.

5. Results

5.1. Experimental Settings

Models and Evaluation. We evaluate our approach on several decoder-based LLMs, including LLaMA2 7B and 13B (Touvron et al., 2023b), Mistral 7B v0.1 (Jiang et al., 2023), and Qwen1.5-7B(Qwen Team, 2024). Language

modeling performance is measured by perplexity on Wiki-Text2 (Merity et al., 2016). Downstream performance is evaluated using the EleutherAI LM Evaluation Harness (Gao et al., 2024) on an aggregate of six tasks: 5-shot MMLU, 0-shot ARC Challenge, 0-shot HellaSwag, 0-shot PIQA, 0-shot BOOLQ and 10-shot WinoGrande (Hendrycks et al., 2021; Clark et al., 2018; Zellers et al., 2019; Bisk et al., 2019; Sakaguchi et al., 2019; Clark et al., 2019).

Baselines. We primarily compare ActTail against TEAL(ICLR’2025)(Liu et al., 2025a), a recent state-of-the-art activation sparsity method, which is training free without any finetuning. To ensure a fair and controlled comparison, we use its TopK formulation with uniform sparsity allocation across projections. We report model-level sparsity for all methods. We do not include TEAL’s threshold-based version, as its input-dependent sparsity leads to varying effective sparsity levels across inputs, which prevents a controlled comparison at matched sparsity budgets.

5.2. Main Results

Language Modeling. Table 1 reports perplexity on Wiki-Text2 for LLaMA2, Mistral, and Qwen1.5 under different activation sparsity levels. ActTail consistently outperforms uniform Top- K allocation across all models, with the advantage becoming increasingly pronounced as sparsity grows. At 70% sparsity, ActTail reduces perplexity by 13.5% on LLaMA2-7B, 9.2% on LLaMA2-13B, 1.8% on Mistral-7B, and 7.2% on Qwen1.5-7B relative to uniform allocation. The gains further amplify at 80% sparsity, where ActTail achieves perplexity reductions of 21.8% on LLaMA2-7B, 40.1% on LLaMA2-13B, and 9.4% on Mistral-7B, while still providing a consistent 1.8% improvement on Qwen1.5-7B. These results demonstrate that heavy-tail-guided projection-level sparsity allocation is particularly effective in the high-sparsity regime, where uniform heuristics incur substantial degradation.

Downstream Tasks. ActTail consistently improves downstream accuracy over uniform activation sparsity on LLaMA2-7B, LLaMA2-13B, Mistral-7B and Qwen1.5-7B across a diverse set of reasoning and knowledge benchmarks, including MMLU, ARC-c, HellaSwag, BOOLQ, PIQA and WinoGrande (Table 2). At 70% sparsity, ActTail improves the averaged score by 3.6% on LLaMA2-7B and by 7.1% on LLaMA2-13B relative to uniform Top- K sparsification. Similar performance gains are also observed on Mistral-7B and Qwen1.5-7B. The performance advantage of ActTail remains evident at 80% sparsity. At 80% sparsity, ActTail improves the averaged performance by 2.9% on LLaMA2-7B, 8.0% on LLaMA2-13B, and 2.1% on Mistral-7B relative to uniform ones. Among all evaluated benchmarks, ActTail exhibits the most pronounced improvements on BOOLQ.

Specifically, ActTail improves BOOLQ accuracy by 27.6% on LLaMA2-7B, 24.6% on LLaMA2-13B, and 16.3% on Mistral-7B at 80% sparsity. Overall, these results confirm that leveraging heavy-tailed spectral heterogeneity enables more robust activation sparsity, yielding superior accuracy and efficiency trade-offs across model sizes and task types.

5.3. Empirical Analysis of Heavy-Tailed Metrics and Activation Sparsity

To better understand how the heavy-tailed self-regularization (HT-SR) metric influences activation sparsity decisions in practice, we analyze the relationship between the estimated heavy-tail exponent α and the resulting sparsity ratios across projections. Figure 5 provides a global view of projection-level α and sparsity ratios, while Figure 4 groups them by module type (Q, K, V, O, Gate, Up, Down) for module-wise comparison. Several clear patterns emerge from this analysis.

First, projections with smaller α values are assigned lower activation sparsity, as heavier-tailed projections encode more concentrated representations that are less tolerant to aggressive sparsification. Second, sparsity allocation varies systematically across module types. Attention projections, especially Q and O, tend to have smaller α values and receive lower sparsity, whereas MLP projections (Gate, Up, Down) show larger α values and tolerate higher sparsity. This explains the suboptimality of uniform or layerwise sparsity schemes. Finally, sparsity closely follows the variation of α across depth rather than remaining constant, indicating that the proposed allocation adapts across both layers and projection types.

6. Conclusion

ActTail uses Heavy-Tailed Self-Regularization theory to show that different projections have different spectral behavior, and uses this to set TopK input activation sparsity per projection. We give theory linking heavy-tailed spectral statistics to projection sparsifiability, explaining why heavier-tailed projections can be sparsified more aggressively with limited loss. Experiments on multiple large language model families show consistent gains in perplexity and downstream performance at high sparsity, supporting HT-SR as a practical basis for theory-guided activation sparsity.

Impact Statement

This paper presents work whose goal is to advance the field of machine learning. There are many potential societal consequences of this work, none of which we believe require specific discussion beyond those commonly associated with research on large language model efficiency.

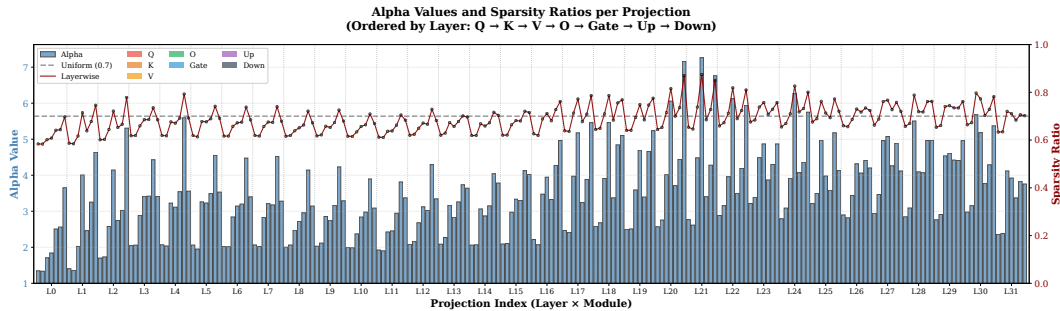


Figure 5. Alpha values and sparsity ratios per projection, ordered by layer and module type (Q, K, V, O, Gate, Up, Down).

References

- Alizadeh, K., Mirzadeh, S. I., Belenko, D., Khatamifard, S., Cho, M., Del Mundo, C. C., Rastegari, M., and Farajtabar, M. Llm in a flash: Efficient large language model inference with limited memory. In *Proceedings of the 62nd Annual Meeting of the Association for Computational Linguistics (Volume 1: Long Papers)*, pp. 12562–12584, 2024.
- An, Y., Zhao, X., Yu, T., Tang, M., and Wang, J. Fluctuation-based adaptive structured pruning for large language models. *Proceedings of the AAAI Conference on Artificial Intelligence*, 38(10):10865–10873, March 2024. ISSN 2374-3468.
- Ashkboos, S., Croci, M. L., do Nascimento, M. G., Hoefler, T., and Hensman, J. SliceGPT: Compress large language models by deleting rows and columns. In *The Twelfth International Conference on Learning Representations*, 2024. URL <https://openreview.net/forum?id=vXxardq6db>.
- Bengio, E., Bacon, P.-L., Pineau, J., and Precup, D. Conditional computation in neural networks for faster models, 2016. URL <https://arxiv.org/abs/1511.06297>.
- Bingham, N. H., Goldie, C. M., and Teugels, J. L. *Regular Variation*, volume 27 of *Encyclopedia of Mathematics and its Applications*. Cambridge University Press, Cambridge, 1987. ISBN 978-0521307870.
- Bisk, Y., Zellers, R., Bras, R. L., Gao, J., and Choi, Y. Piqa: Reasoning about physical commonsense in natural language, 2019. URL <https://arxiv.org/abs/1911.11641>.
- Clark, C., Lee, K., Chang, M.-W., Kwiatkowski, T., Collins, M., and Toutanova, K. Boolq: Exploring the surprising difficulty of natural yes/no questions. In *Proceedings of the 2019 Conference of the North American Chapter of the Association for Computational Linguistics: Human Language Technologies, Volume 1 (Long and Short Papers)*, pp. 2924–2936, 2019.
- Clark, P., Cowhey, I., Etzioni, O., Khot, T., Sabharwal, A., Schoenick, C., and Tafjord, O. Think you have solved question answering? try arc, the ai2 reasoning challenge, 2018. URL <https://arxiv.org/abs/1803.05457>.
- Couillet, R. and Liao, Z. *Random matrix methods for machine learning*. Cambridge University Press, 2022.
- DeVore, R. A. Nonlinear approximation. In *Acta Numerica 1998*, volume 7 of *Acta Numerica*, pp. 51–150. Cambridge University Press, 1998. doi: 10.1017/S0962492900002816.
- Frantar, E. and Alistarh, D. Sparsegpt: Massive language models can be accurately pruned in one-shot, March 2023.
- Gao, L., Tow, J., Abbasi, B., Biderman, S., Black, S., DiPofi, A., Foster, C., Golding, L., Hsu, J., Le Noac’h, A., Li, H., McDonnell, K., Muennighoff, N., Ociepa, C., Phang, J., Reynolds, L., Schoelkopf, H., Skowron, A., Sutawika, L., Tang, E., Thite, A., Wang, B., Wang, K., and Zou, A. A framework for few-shot language model evaluation, 07 2024. URL <https://zenodo.org/records/12608602>.
- He, D., Tu, S., Jaiswal, A., Shen, L., Yuan, G., Liu, S., and Yin, L. Alphadecay: Module-wise weight decay for heavy-tailed balancing in LLMs. In *The Thirty-ninth Annual Conference on Neural Information Processing Systems*, 2025. URL <https://openreview.net/forum?id=MKEDsVWHd0>.
- Hendrycks, D., Burns, C., Basart, S., Zou, A., Mazeika, M., Song, D., and Steinhardt, J. Measuring massive multitask language understanding, 2021. URL <https://arxiv.org/abs/2009.03300>.

- Hill, B. M. A simple general approach to inference about the tail of a distribution. *The Annals of Statistics*, 3(5): 1163–1174, 1975. ISSN 00905364, 21688966. URL <http://www.jstor.org/stable/2958370>.
- Hoffmann, J., Borgeaud, S., Mensch, A., Buchatskaya, E., Cai, T., Rutherford, E., de Las Casas, D., Hendricks, L. A., Welbl, J., Clark, A., Hennigan, T., Noland, E., Millican, K., van den Driessche, G., Damoc, B., Guy, A., Osindero, S., Simonyan, K., Elsen, E., Vinyals, O., Rae, J., and Sifre, L. An empirical analysis of compute-optimal large language model training. In Koyejo, S., Mohamed, S., Agarwal, A., Belgrave, D., Cho, K., and Oh, A. (eds.), *Advances in Neural Information Processing Systems*, volume 35, pp. 30016–30030. Curran Associates, Inc., 2022.
- Huang, X., Huang, Y.-L., and Wen, Z. Sola: Leveraging soft activation sparsity and low-rank decomposition for large language model compression. *Proceedings of the AAAI Conference on Artificial Intelligence*, 39(16):17494–17502, Apr. 2025. doi: 10.1609/aaai.v39i16.33923. URL <https://ojs.aaai.org/index.php/AAAI/article/view/33923>.
- Jahn, T. and Ullrich, T. On the optimal constants in the two-sided Stechkin inequalities. *Journal of Approximation Theory*, 269:105607, 2021. doi: 10.1016/j.jat.2021.105607.
- Jiang, D., Liu, Y., Liu, S., Zhao, J., Zhang, H., Gao, Z., Zhang, X., Li, J., and Xiong, H. From clip to dino: Visual encoders shout in multi-modal large language models. *arXiv preprint arXiv:2310.08825*, 2023.
- Kaplan, J., McCandlish, S., Henighan, T., Brown, T. B., Chess, B., Child, R., Gray, S., Radford, A., Wu, J., and Amodei, D. Scaling laws for neural language models, 2020. URL <https://arxiv.org/abs/2001.08361>.
- Lee, D., Lee, J., Zhang, G., Tiwari, M., and Mirhoseini, A. Cats: Context-aware thresholding for sparsity in large language models. In *First Conference on Language Modeling*, August 2024.
- Li, Z., You, C., Bhojanapalli, S., Li, D., Rawat, A. S., Reddi, S. J., Ye, K., Chern, F., Yu, F., Guo, R., and Kumar, S. The lazy neuron phenomenon: On emergence of activation sparsity in transformers. In *The Eleventh International Conference on Learning Representations*, 2023. URL <https://openreview.net/forum?id=TJ2nxcYck->.
- Ling, G., Wang, Z., YuliangYan, and Liu, Q. SlimGPT: Layer-wise structured pruning for large language models. In *The Thirty-eighth Annual Conference on Neural Information Processing Systems*, 2024. URL <https://openreview.net/forum?id=MxF0IKJtKW>.
- Liu, J., Ponnusamy, P., Cai, T., Guo, H., Kim, Y., and Athiwaratkun, B. Training-free activation sparsity in large language models, February 2025a.
- Liu, K., Xu, B., Wu, S., Chen, X., Zhou, H., Tao, Y., and Hu, L. La rosa: Enhancing llm efficiency via layerwise rotated sparse activation, July 2025b.
- Liu, Z., Wang, J., Dao, T., Zhou, T., Yuan, B., Song, Z., Shrivastava, A., Zhang, C., Tian, Y., Re, C., and Chen, B. Deja vu: Contextual sparsity for efficient llms at inference time. In *Proceedings of the 40th International Conference on Machine Learning*, pp. 22137–22176. PMLR, July 2023.
- Lu, H., Zhou, Y., Liu, S., Wang, Z., Mahoney, M. W., and Yang, Y. Alphapruning: Using heavy-tailed self regularization theory for improved layer-wise pruning of large language models, October 2024.
- Martin, C. H. and Mahoney, M. W. Rethinking generalization requires revisiting old ideas: statistical mechanics approaches and complex learning behavior, 2017.
- Martin, C. H. and Mahoney, M. W. Traditional and heavy tailed self regularization in neural network models. In *International Conference on Machine Learning*, 2019.
- Martin, C. H. and Mahoney, M. W. Heavy-tailed universality predicts trends in test accuracies for very large pre-trained deep neural networks. In *SIAM International Conference on Data Mining*, 2020.
- Martin, C. H. and Mahoney, M. W. Post-mortem on a deep learning contest: a Simpson’s paradox and the complementary roles of scale metrics versus shape metrics, 2021a.
- Martin, C. H. and Mahoney, M. W. Implicit self-regularization in deep neural networks: Evidence from random matrix theory and implications for learning. *Journal of Machine Learning Research*, 22(165):1–73, 2021b.
- Martin, C. H., Peng, T. S., and Mahoney, M. W. Predicting trends in the quality of state-of-the-art neural networks without access to training or testing data. *Nature Communications*, 12(1):4122, July 2021. ISSN 2041-1723.
- Merity, S., Xiong, C., Bradbury, J., and Socher, R. Pointer sentinel mixture models. *arXiv preprint arXiv:1609.07843*, 2016.
- Mirzadeh, S. I., Alizadeh-Vahid, K., Mehta, S., del Mundo, C. C., Tuzel, O., Samei, G., Rastegari, M., and Farajtabar, M. Relu strikes back: Exploiting activation sparsity in large language models, 2023.

- Qwen Team. Introducing qwen1.5, February 2024. URL <https://qwenlm.github.io/blog/qwen1.5/>.
- Resnick, S. I. *Extreme Values, Regular Variation, and Point Processes*, volume 4 of *Applied Probability*. Springer, New York, 1987. ISBN 978-0387960812. doi: 10.1007/978-1-4757-2099-8.
- Sakaguchi, K., Bras, R. L., Bhagavatula, C., and Choi, Y. Winogrande: An adversarial winograd schema challenge at scale, 2019. URL <https://arxiv.org/abs/1907.10641>.
- Shen, X., Song, Z., Zhou, Y., Chen, B., Liu, J., Zhang, R., Rossi, R. A., Tan, H., Yu, T., Chen, X., et al. Numerical pruning for efficient autoregressive models. In *Proceedings of the AAAI Conference on Artificial Intelligence*, volume 39, pp. 20418–20426, 2025.
- Shrestha, S., Settlemeyer, B., Dryden, N., and Reddy, N. Polar sparsity: High throughput batched llm inferencing with scalable contextual sparsity, November 2025.
- So, D., Mañke, W., Liu, H., Dai, Z., Shazeer, N., and Le, Q. V. Searching for efficient transformers for language modeling. *Advances in neural information processing systems*, 34:6010–6022, 2021.
- Song, Y., Mi, Z., Xie, H., and Chen, H. Powerinfer: Fast large language model serving with a consumer-grade gpu. In *Proceedings of the ACM SIGOPS 30th Symposium on Operating Systems Principles*, pp. 590–606, 2024.
- Sun, M., Liu, Z., Bair, A., and Kolter, J. Z. A simple and effective pruning approach for large language models. In *The Twelfth International Conference on Learning Representations*, 2024. URL <https://openreview.net/forum?id=PxoFut3dWW>.
- Touvron, H., Martin, L., Stone, K., Albert, P., Almahairi, A., Babaei, Y., Bashlykov, N., Batra, S., Bhargava, P., Bhosale, S., et al. Llama 2: Open foundation and fine-tuned chat models. *arXiv preprint arXiv:2307.09288*, 2023a.
- Touvron, H., Martin, L., Stone, K., Albert, P., Almahairi, A., Babaei, Y., Bashlykov, N., Batra, S., Bhargava, P., Bhosale, S., et al. Llama 2: Open foundation and fine-tuned chat models. *arXiv preprint arXiv:2307.09288*, 2023b.
- van der Vaart, A. W. *Asymptotic Statistics*. Cambridge University Press, Cambridge, 1998. ISBN 978-0521784503. doi: 10.1017/CBO9780511802256.
- Vershynin, R. *High-Dimensional Probability: An Introduction with Applications in Data Science*. Cambridge Series in Statistical and Probabilistic Mathematics. Cambridge University Press, Cambridge, 2018. doi: 10.1017/9781108231596.
- Wang, X., Zheng, Y., Wan, Z., and Zhang, M. SVD-LLM: Truncation-aware singular value decomposition for large language model compression. In *The Thirteenth International Conference on Learning Representations*, 2025. URL <https://openreview.net/forum?id=LNyIUouhdt>.
- Xiao, X., Li, Z., Xie, C., and Zhou, F. Heavy-tailed regularization of weight matrices in deep neural networks, 2023. URL <https://arxiv.org/abs/2304.02911>.
- Yang, A., Li, A., Yang, B., Zhang, B., Hui, B., Zheng, B., Yu, B., Gao, C., Huang, C., Lv, C., et al. Qwen3 technical report. *arXiv preprint arXiv:2505.09388*, 2025.
- Yang, Y., Theisen, R., Hodgkinson, L., Gonzalez, J. E., Ramchandran, K., Martin, C. H., and Mahoney, M. W. Test accuracy vs. generalization gap: Model selection in nlp without accessing training or testing data. In *Proceedings of the 29th ACM SIGKDD Conference on Knowledge Discovery and Data Mining*, pp. 3011–3021, 2023.
- Zellers, R., Holtzman, A., Bisk, Y., Farhadi, A., and Choi, Y. Hellaswag: Can a machine really finish your sentence?, 2019. URL <https://arxiv.org/abs/1905.07830>.
- Zhang, Z., Song, Y., Yu, G., Han, X., Lin, Y., Xiao, C., Song, C., Liu, Z., Mi, Z., and Sun, M. Relu² wins: Discovering efficient activation functions for sparse llms. *arXiv preprint arXiv:2402.03804*, 2024.
- Zhang, Z., Liu, Z., Tian, Y., Khaitan, H., Wang, Z., and Li, S. R-sparse: Rank-aware activation sparsity for efficient llm inference, April 2025.
- Zhou, Y., Pang, T., Liu, K., charles h martin, Mahoney, M. W., and Yang, Y. Temperature balancing, layer-wise weight analysis, and neural network training. In *Thirty-seventh Conference on Neural Information Processing Systems*, 2023. URL <https://openreview.net/forum?id=oyV9Fs1E3j>.